ELSEVIER

Thermochimica Acta 379 (2001) 101–109

thermochimica acta

www.elsevier.com/locate/tca

Influence of preparation method on thermal stability and acidity of Al–PILCs

P. Salerno*, M.B. Asenjo, S. Mendioroz

Instituto de Catálisis y Petroleoquimica, CSIC, Campus de la UAM, Cantoblanco, 28049 Madrid, Spain

Abstract

In general, clays may be modified introducing hydroxications between the constituent layers to obtain microporous solids, known as pillared clays (PILCs), useful in adsorption and catalysis. In this work, XRD, FT-IR, N_2 adsorption isotherms and ammonia adsorption techniques were applied to study the changes in structure and properties provided to a montmorillonite through pillaring when different preparation methods, Al/clay ratio and drying procedures are used in the synthesis. Above a certain Al/clay ratio, pillar density is addressed by the maximum exchange capacity of the clay at the pH of the pillaring solution. Under such a situation, micro- and meso-porosity remain almost unchanged whereas macroporosity is fully dependent on the concentration of the clay suspension and more on the drying conditions of the flocculated exchanged clay layers. Thermal analysis has shown as a useful tool to understand the changes in acidity with the temperature.

Keywords: Alumina pillared clays; Slurry method; Pillar density; Ammonia adsorption

1. Introduction

Pillared clays have reached considerable interest as catalysts and catalysts supports over the past years. Their porosity, reactivity and thermal stability are being widely applied in adsorption and catalysis [1,2]. Concerning catalysis, those materials (PILCs) are being used in a wide range of reactions [3–16].

As it is known, the number of ionic precursors and, thus, of eventual number of pillars introduced in a clay is dependent on the cation exchange capacity (CEC) of the clay and the charge of the ionic precursor. Montmorillonite, a phyllosilicate of the smectite group, is currently used as host material because its relatively high CEC that guarantees the stability of the obtained materials. Metals commonly used as ionic precursors are Al [17,18], Fe [17,19,20], Zr [19–21], Cr [19,20,22], Ti [22], Ga [3,23]. Among them, aluminium has been profusely used as pillaring agent due to its hydrolisis capability to form large inorganic polymeric oxy-hydroxy cations of several nuclearities. The major aluminium species used is the $[Al_{13}]^{7+}$ polymer but other mono and polynuclear species may be present in solution depending on its pH [6]. The actual exchange is dependent, as in every diffusion process, on the pillaring agent solution concentration and the ageing conditions of the formed cation whose size and charge (n/q ratio) deeply depends on the synthesis conditions. Also, the effect of the drying method is claimed to be more important than the pillaring reagent itself or even the clay layer charge on PILCs pore opening, giving rise to products with uniform pore size when air-dried or with a continuous distribution of larger pores when freeze-dried. With all that in mind, the possibility of tuning the properties

* Corresponding author.

0040-6031/01/$ – see front matter
PII: S0040-6031(01)00608-6

of PILCs by varying the synthesis conditions seems plausible [24,25].

In general, the pillaring processes are carried out in diluted systems, less than 2 wt.% of clay suspension and less than 0.5 M of pillaring solution [5,6]. When a large amount of materials has to be prepared, a quite large volume of solutions has to be handled which turns the PILCs synthesis in a non-viable industrial method. Vaugan [26] proposed the first approaches to prepare PILCs in large quantities. More recently, a method of synthesis based on the use of highly concentrated clay suspensions without any previous purification or homoionisation of clay prior to pillaring has been developed [17]. The method enables the preparation of industrial quantities of pillared materials with uniform properties, and its scale-up seems promising. However, only scarce information has been, up to the moment, reported on the physico-chemical characteristics of the resulting materials and on their comparison with those obtained by the more conventional method of diluted suspensions.

The present paper deals with the preparation of pillared clays from concentrated montmorillonite suspensions under two Al/clay ratios and their comparison with those resulting from diluted systems at the same Al/clay ratio. Also the effect of the drying procedure will be studied.

2. Experimental

2.1. Raw material

A montmorillonite from La Serrata de Nijar, Spain, was used. Characterisation studies show that it was a dioctahedral, high purity, and iron rich montmorillonite, with Ca, Mg and Na as the main exchangeable cations. The structural formula calculated from chemical analysis and cation exchange capacity measurements (CEC = 119 meq/100 g) was

$$M_{0.824}{}^{+}[Al_{2.642} \cdot Fe_{0.512} \cdot Mg_{0.782} \cdot Mn_{0.008}] \times [Si_{7.906} \cdot Al_{0.094}]O_{24.708}OH_{4.942}$$

Physico-chemical characteristics were: surface area, (S_{BET}) 81 m^2/g, total pore volume (V_{total}), 0.744 cm^3/g, acidity measured by NH_3 adsorption at room temperature, 0.76 meq NH_3/g.

2.2. Preparation method

2.2.1. Method 1

The mineral, as such, was suspended in water in a 2 wt.% concentration. A 0.2 M $AlCl_3{\cdot}6H_2O$ solution treated with a 0.5 M NaOH solution as hydrolysing agent in an OH/Al molar ratio of 2, aged and refluxed during 24 h at 363 K was used as Al-pillaring agent. The aged solution was added drop-wise to the clay suspension and stirred for 4 h. The solid was separated by decantation, dialysed till chloride free, dried at 353 K and heat treated in static atmosphere at 773 K for 2 h.

2.2.2. Method 2

Pillared clays were prepared on the basis of the ''slurry'' method described in literature [17]. In this case, a 50% aqueous solution of Locron® (a form of Al keggin cation commercialised by Hoechst) was used as pillaring agent. This solution was added drop-wise to a 50 wt.% natural clay suspension in acetone and stirred during 1 h. The final suspension, after decantation, was dialysed against distilled water until chloride free. A fraction of the final product was dried at 353 K and another was freeze-dried. Both fractions were equally heat treated at 773 K for 2 h to fix the cation to the clay, converted to metal oxide cluster.

Materials obtained by Method 1 were labelled as Al(x) and those obtained by Method 2, as Loc(x) and Lio(x) when heat dried and freeze-dried, respectively. Here x means the number of meq Al per gram clay used in the pillaring solution that, in this work, were 20 and 30.

2.3. Analysis techniques

X-ray powder diffraction patterns were obtained at room temperature in a Seifert-XRD 3000 under 40 kV, 40 mA current intensity in the 2θ (2–20°) range at 0.02°/min and Cu Kα irradiated.

FT-IR spectra were taken in a Nicolet model 5ZDX spectrophotometer in the 4000–400 cm^{-1} range. The detector was a MCT type. The samples were prepared by the KBr technique.

BET surface area, volumes of micro- and mesopores were obtained from N_2 adsorption–desorption isotherms at 77 K, measured in a Micromeritics ASAP 2010 on samples outgassed at 613 K. As N_2 cross-sectional area 0.16 nm^2 was always taken. For

porosity analysis, the BJH method [27] and the *H–J* standard curve [28] were used. Macroporosity was evaluated with a conventional mercury intrusion apparatus (Fisons with Pascal 140 and Pascal 240 modules).

Thermal analysis was effected in a TGS2 thermobalance with DS 3700 and temperature controller system 7/4 from Perkin-Elmer. The equipment sensitivity was less than 0.2 μg. For acidity evaluation, ammonia adsorption was effected after degassing the sample for 2 h under flowing N_2 at 673 K. Once cooled at room temperature, the degassed sample as 100 wt.% was exposed to a 100 cm^3/min gas flow of 50% NH_3 in N_2 until equilibrium (around 120 min). Afterwards, NH_3 was turned off and N_2 left to flow to clean the sample from the physisorbed ammonia until equilibrium (around 360 min). Finally, the sample was heated at 10 K/min rate up to 633 K and the retained NH_3 at selected temperatures evaluated.

3. Results

3.1. X-ray diffractograms

Fig. 1 shows the same basal spacing for all samples, around 18 Å, denoting the incorporation of a similar type of oxocations 9 Å size [29], probably the $[Al_{13}]^{7+}$ cation, independently of the preparation method used.

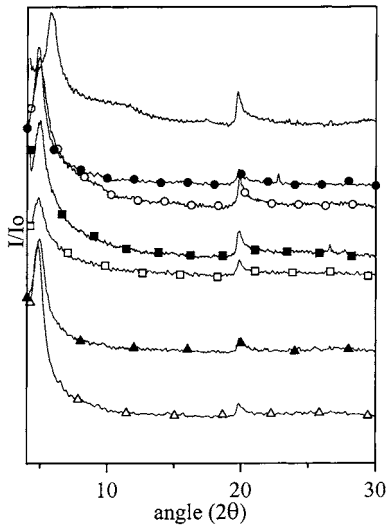

Fig. 1. XRD of parent and pillared clays. Clay (no-symbol); Al20 (○); Al30 (●); Loc20 (□); Loc30 (■); Lio20 (△); Lio30 (▲).

However, some differences in peaks intensities and width are visible pointing to slight differences in the stacking and/or crystallinity degree among the samples prepared by different methods and Al/clay ratios.

3.2. FT-IR spectra

The infrared spectrum of the parent clay in Fig. 2 exhibits two peaks at 3440 and 3660 cm^{-1} at the OH

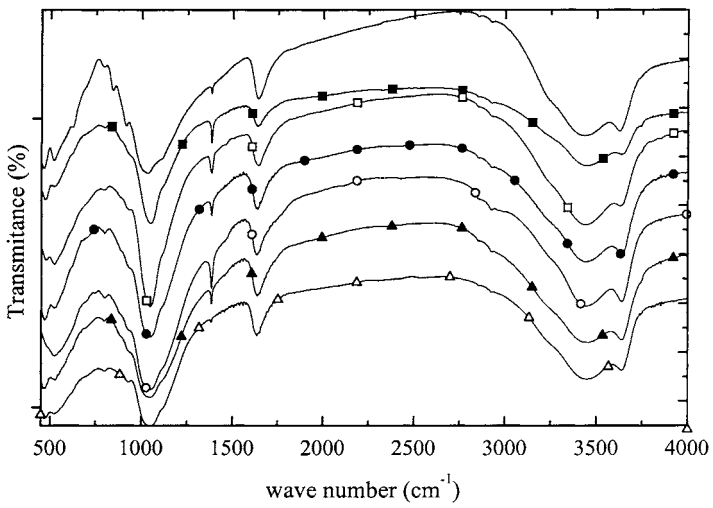

Fig. 2. FT-IR of parent and pillared clays. Clay (no-symbol); Al20 (○); Al30 (●); Loc20 (□); Loc30 (■); Lio20 (△); Lio30 (▲).

stretching region. The pattern is typical of water adsorption in montmorillonite [30,31] and is ascribed to the –OH stretching vibration in Al_2OH hydroxyl absorption of randomly oriented samples, and to hydroxyl groups involved in water–water hydrogen bonds, respectively. A shoulder around 3250 cm^{-1} can be ascribed to an overtone of the water bending vibration visible at 1645 cm^{-1}.

A broad peak around 1020 cm^{-1} is assigned to the in-plane stretching vibration of surface Si–O–Si when substitution of Si by Al is low. Al_2OH libration lies in the 910 cm^{-1} range and Mg substitution for Al (in MgAlOH) at 840 cm^{-1}. Finally a peak at 720 cm^{-1} altogether with those at 520 and 460 cm^{-1} can be associated to Si–O bending vibration [31,32].

Concerning to pillared samples, an increase in the 3440 cm^{-1}/3660 cm^{-1} intensities ratio is visible with respect to the parent clay, much important on Al(x) and Loc(x) series than on Lio(x) series.

When the surface charge is concentrated on oxygen involved in Si–O–Si linkages, the OH groups hydrogen bonded to those oxygens, absorb near 3440 cm^{-1} overlapping the region of absorption associated to water–water linkages, enhancing the 3440 cm^{-1} peak intensity relative to the 3440 cm^{-1} peak [31,32]. This intensities increase in the 3440 cm^{-1} peak could be related to the presence of aluminium oxocations in the samples, forming pillars or not.

Also a shift of the 1020 cm^{-1} peak of the parent clay towards higher frequencies nearly the same in all samples (1045 cm^{-1}) is visible. This fact has been related to a change in the symmetry of the surface Si–O–Si vibration perhaps associated to a change in the electric field near the Si groups due to the proximity of more positively charged aluminium groups. The bands at 910 and 840 cm^{-1} decrease with pillaring but no important differences among samples are visible, denoting a similar degree of exchange.

Finally a band at 1380 cm^{-1} appears in all samples. This band can be assigned to carbonates or bicarbonates formed with the remaining exchangeable cations (mainly Ca and/or K) at ambient conditions and, therefore, independent of the synthesis conditions.

3.3. Surface area and porosity

Fig. 3(a) and (b) show the N_2 adsorption–desorption isotherms corresponding to pillared samples and parent material. Always a type IV curve with H4 hysteresis loop was found, denoting a slit-shaped porosity between plate-like particles [33]. The feature of all curves is the same, the only noticeable differences

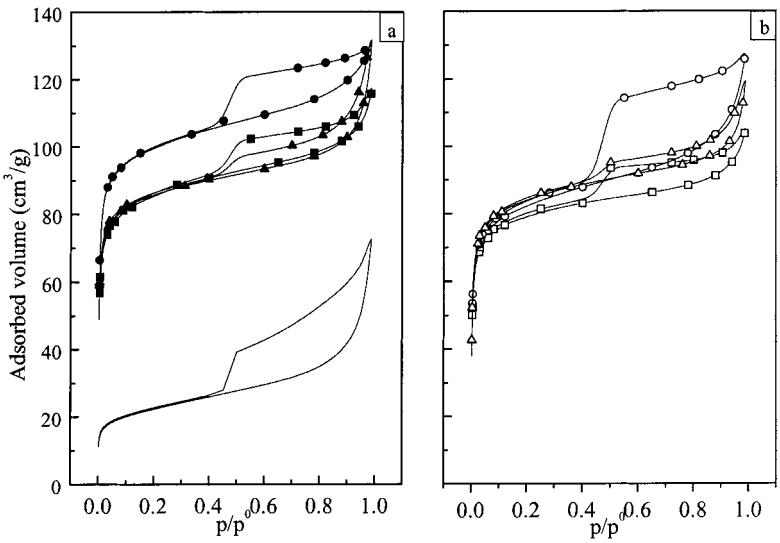

Fig. 3. Nitrogen adsorption–desorption isotherms of (a) parent clay, 30 and (b) 20 series. Clay (no-symbol); Al20 (○); Al30 (●); Loc20 (□); Loc30 (■); Lio20 (△); Lio30 (▲).

Table 1
Main physico-chemical characteristics of the samples

	Sample						
	Clay	Al20	Al30	Loc20	Loc30	Lio20	Lio30
$d_{(0\,0\,1)}$	15[a]	18.4	18.1	18.2	18.0	18.1	18.0
CEC (meq/100 g)	119	20	21	20	21	–	–
S_{BET} (cm^2/g)	81	310	374	298	320	317	322
$V_{\mu p}$ (cm^3/g)	0.013	0.092	0.112	0.089	0.090	0.091	0.098
V_{mp} (cm^3/g)	0.061	0.059	0.064	0.046	0.059	0.047	0.052
V_M (cm^3/g)	0.683	0.212	0.486	0.674	0.881	0.619	1.000
V_{total} (m^3/g)	0.744	0.271	0.550	0.720	0.940	0.666	1.052

[a] Hydrated at room conditions.

being in the first part of the isotherms, below $0.4p/p^0$, corresponding to adsorption in micropores, and in the last part, above $0.9p/p^0$, corresponding to macropores. The extension of the hysteresis loops is the same being slightly wider on Al(x) than on the remaining samples.Table 1 summarises the values for surface area and pore volumes obtained from applying the BET equation and the BJH method, respectively to the proper data in the isotherm. Microporosity has been evaluated from application of t-method [34] to the data below $0.1p/p^0$ using as t width the statistical curve of Harkins and Jura [28].

From the isotherms, it is clear that pillaring generates an important amount of micropores in the clay, almost the same for all samples, regardless the method, Al/clay ratio and drying procedure used. Only a slight increase in S_{BET}, not higher than 10% is visible on Al30. The same occurs with mesoporosity. In general, micro- ($V_{\mu p}$) and meso-pore (V_{mp}) volumes are not affected by the preparation method provided that the Al/clay ratio is high enough to produce total exchange in the clay (see CEC on Table 1).

The contrary happens with macroporosity (V_M), which is dramatically affected by the variables studied. In that sense, 30 series shows a larger pore volume than 20 series whichever the method used (see V_M and V_{total} in Table 1), the differences among samples increasing when higher concentration of the

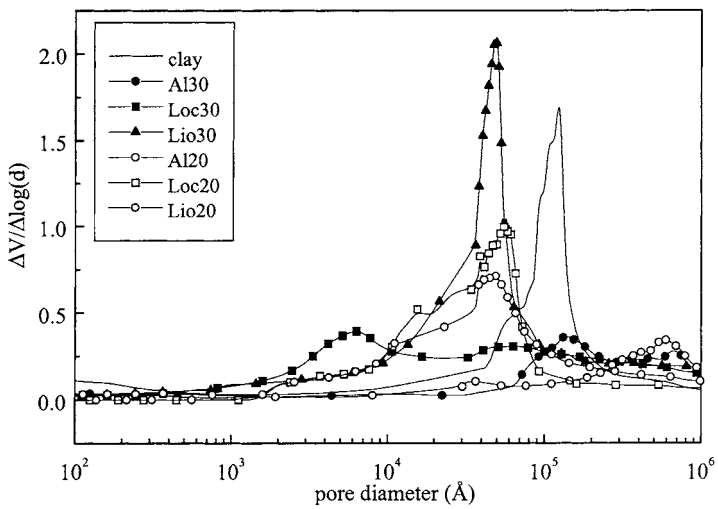

Fig. 4. Pores distribution of parent and pillared clays. Clay (no-symbol); Al20 (○); Al30 (●); Loc20 (□); Loc30 (■); Lio20 (△); Lio30 (▲).

starting clay suspension and freeze-drying instead of air-drying are used. Also macropore size is affected. Thus, in Al(x) series inter-particle voids of diameter around 60 μm are found, whereas 3 μm is the dominant size in Loc(x) series (see Fig. 4). Also 30 series results in a slightly smaller pore size than 20 series probably caused the presence of an excess of aluminium hindering the pores entry.

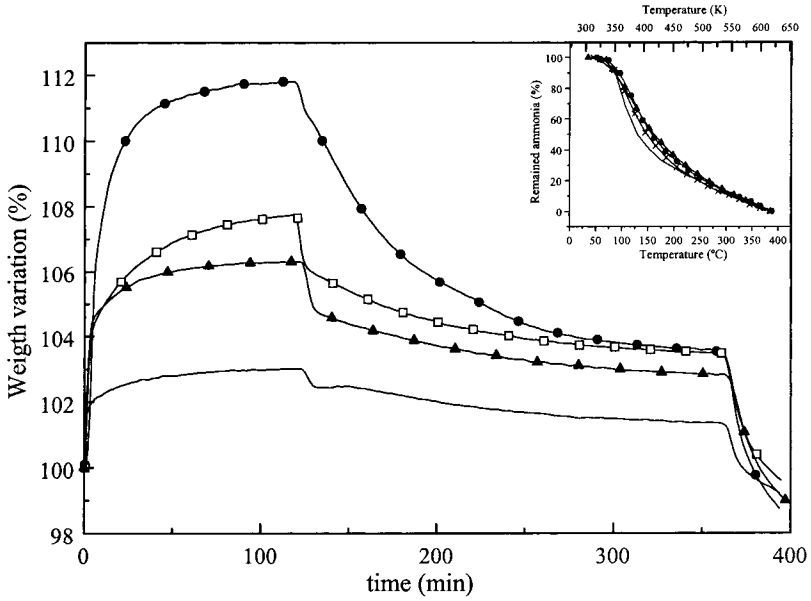

(a)

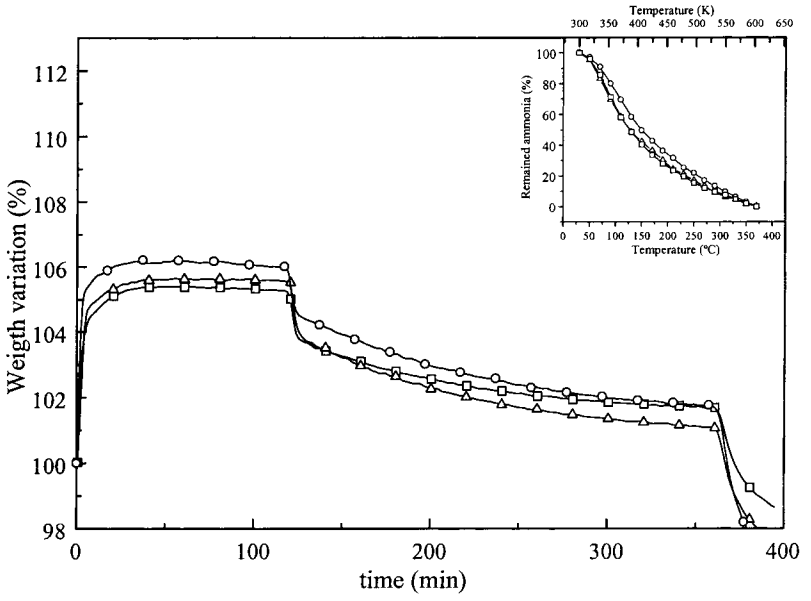

(b)

Fig. 5. Sorption of (a) parent clay, 30 and (b) 20 series. Clay (no-symbol); Al20 (○); Al30 (●); Loc20 (□); Loc30 (■); Lio20 (△); Lio30 (▲).

Table 2
Acidity of the samples by ammonia chemisorption

Sample	Acidity (meq/g)	Acidity distribution (% NH_3 remained in sample)				
		RT (K)	373 (K)	473 (K)	573 (K)	623 (K)
Clay	0.76	100	76	28	12	5
Al20	1.02	100	75	34	12	3
Al30	2.11	100	88	33	13	6
Loc20	0.98	100	64	26	8	2
Loc30	2.01	100	74	27	10	3
Lio20	0.60	100	64	27	7	2
Lio30	1.65	100	82	36	13	5

3.4. Acidity

Ammonia adsorption on PILCs, Fig. 5(a) and (b), surpasses the value taken up by the parent clay and is much more important in 30 series, doubling the values of 20 series. On the other hand, Lio(x) series adsorbs less ammonia than the corresponding Al(x) and Loc(x) series. It is widely known that ammonia uptake is due to adsorption on acidic centres with a wide range of adsorption activation energies involved. After swept off the weakly adsorbed ammonia by N_2 stream, the retained fraction, expressed as meq of ammonia adsorbed per gram, is indicative of the number of acidic centres of the sample.

The inserted figures on the top-right corner of Fig. 5(a) and (b) represent the percent amount of ammonia retained at each temperature. Calculated data from them are summarised in Table 2. As can be seen, pillaring strongly increases the acidity of the parent material, the Al/clay ratio playing an important role in that increase.

4. Discussion

Neither the synthesis method nor the Al/clay ratio used in the synthesis impart important differences in structure to the obtained products, as has been shown by X-ray diffractograms and FT-IR spectra. Only an increase in the coordinated hydration water on Al(x) series, probably related to the nature of the pillaring cations, and a relative decrease on Lio(x) series, as a consequence of the drying method has been detected. On the other hand, the values for CEC (Table 1), the same for all samples, suggest that exchange reach a constant value, whatever the synthesis conditions, which for this material and under the preparation conditions used in this work, is of about 98 meq/100 g clay. In a previous work (in press), the authors found, for the same parent material, that a similar exchange is reached with no more than 10 meq Al/g clay. That means, that the same number of pillars has incorporated to the clay, independent of the preparation methods and the clay/Al ratio, above a certain value, giving rise to similar values for micro- and meso-porosity in all samples.

However, an excess aluminium must have incorporated to the samples in some way other than forming pillars in order to explain the changes in texture and specially in acidity detected.

Having in mind that one of the synthesis steps for all methods was the repeatedly washing of the samples up to reach the same conductivity in the washing water (50 μS), it must be admitted that Al (probably as oxocation of any type) is bounded to edge sites of the clay in the interlayer or/and on the external surface and plays an important role in the final texture and acidity of the PILCs.

The dependence of pore size on drying method, visible above 3 μm (Fig. 4), is most likely related to the mechanism of layer aggregation. Freeze-drying will preserve the structure of the flocculated clay in suspension, giving rise to edge-to-edge or face-to-edge aggregation, whereas air-drying optimises the face-to-face aggregation. The size of the aggregates, and consequently the size of the voids among aggregates, will depend on the ordered organisation and will be higher on Al(x) than on Loc(x) and specially than on Lio(x) series.

Thus, two are the factors that contribute to the final properties of those samples, the flocculation of the products and the excess aluminium that may act as

joining cement among particles, reinforcing the effect of layer aggregation after drying. All that is confirmed by X-ray diffractograms and also by the extension of the hysteresis loops slightly wider on Al(x).

Concerning ammonia adsorption, Fig. 5, it can be seen that the rate of adsorption differs from sample to sample on 30 series, whereas it is almost the same on 20 series. Saturation takes more time on sample Al30. In general, the ''knee'' in the type 1 curve obtained in the adsorption step shows the following order: Al30 < Loc30 < Lio30. As its known [35], amine adsorption by clays needs an ''induction'' period before the lamellae, on which adsorption is to be effected, open, leaving the remaining amine to penetrate the sample. This effect is not expected on pillared samples, because their structure is completely opened by the pillars. However, it does exist in 30 series, which must be related to the presence of aluminium oxide on the clay edges (being the more active sites) holding up, in part, the entrance of ammonia inwards the clay core. This effect is more important on Al30 due to the preparation method (specially drying) that generates a more ordered structure.

Acidity is strongly affected by pillaring. Fig. 6 represents the differentiated data from the insert in Fig. 5 in function of temperature. In order to compare, natural clay curve was added. As can be seen, peaks intensities and position change in pillared samples with respect to parent clay and among them. On natural clay, three desorption peaks corresponding to weak, medium and strong acid sites are visible. They can be ascribed to isomorphic substitutions in the tetrahedral and octahedral layers (which allow polarisability of the hydrating water and protonisation of structural –OH groups) and coordinatively unsaturated Al located at the terminal octahedral sheet altogether with surface defects by broken bonds [6].

After pillaring an additional peak, visible as a shoulder in some samples, is evident at temperature near 498 K, which must be assigned to the incorporated aluminium. Also differences in peaks intensities and position are produced but the relative contribution to the total acidity is more or less the same.

Acidity is defined not only by the number of acidic sites but also by their type and strength [36]. Then, pillaring affects both Lewis and Brönsted acid sites, not discriminated here. On one hand, it must be realised that the pillaring process involves the separation of the lamellae and consequent exposition of sylanols, some from them liable to become acidic in amine presence. In fact, this is the main source of Brönsted acidity visible up to 373 K. Also, calcination of the pillars in the synthesis step, releases protons as a consequence of –OH condensation between cations and clay and subsequent water evolution, enhancing Brönsted acidity, less in Lio(x) series.

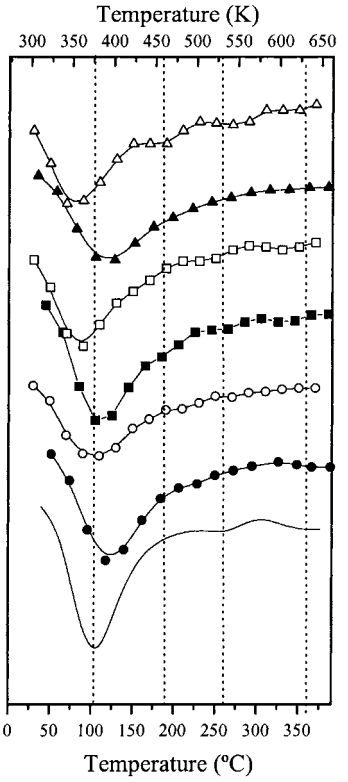

Fig. 6. Differential ammonia release with temperature of parent and pillared clays. Clay (no-symbol); Al20 (○); Al30 (●); Loc20 (□); Loc30 (■); Lio20 (△); Lio30 (▲).

On the other hand, the contribution of pillars to the acidity of PILCs is mainly of Lewis type [37]. The number of pillars is similar in all samples, but the amount of incorporated aluminium not. Then, the excess aluminium oxihydroxide gives rise through calcination to coordinatively unsaturated Al atoms which are also identified as potential Lewis acids and result in an additional increase in the total number of acid centres. In this case, it is clear that the number of acids centres grows in the same sense that the Al/clay ratio and that this increase in number of centres as

much as in strength, must be specially related to the Al content in the samples. It cannot be disregard that Method 1, with the pillaring cation obtained by reflux, probably gives rise to different aluminium polymeric species with higher n/q ratio (number of Al atoms per charge) than the keggin cation, increasing the number of acidic centres [5,36] and providing a stronger acidity to the sample.

5. Conclusions

Pillaring supplies to the parent material, an increase in surface area and porosity, mostly in microporosity, and especially in the number of acid centres.

At the Al/clay ratios used in this work, a complete exchange was reached during pillaring by either method. Then, neither micro- nor meso-porosity are affected by the preparation method, but macroporosity does, playing the drying procedure a more important role in pore sizes than the synthesis method itself or even the Al/clay ratio.

Acidity is increased by pillaring, the number and strength of the formed acid sites being dependent mainly on the Al/clay ratio. The products obtained by the conventional method, show more acidity than those obtained by the slurry method, likely because excess aluminium is located on more orderly placed and ammonia accessible basal surfaces and edge sites, and in air-dried than freeze-dried samples.

The slurry method gives rise to materials with similar properties to those obtained through the more conventional, more time-consuming method of diluted suspensions, opening the way to scale-up the synthesis procedure.

Finally, TGA has shown as a quite useful tool for acidity studies of materials via amine adsorption and thermal desorption but also for helping to understand the structure of the pillared materials.

References

[1] E. Kikuchi, T. Matsuda, Catal. Today 2 (1988) 297.
[2] I. Mrad, A. Ghorbel, D. Tichit, F. Lambert, Appl. Clay Sci. 12 (1997) 349.
[3] K.B. Brandt, R.A. Kydd, Appl. Catal. A 165 (1997) 327.
[4] S. Moreno, E. Gutierrez, A. Alvarez, N.G. Papayanakos, G. Poncelet, Appl. Catal. A 165 (1997) 103.
[5] F. Figueras, Catal. Rev. Sci. Eng. 30 (1988) 457.
[6] J.F. Lambert, G. Poncelet, Topics Catal. 4 (1997) 43.
[7] F. Gonzalez, C. Pesquera, I. Benito, E. Herrero, C. Poncio, S. Casuscelli, Appl. Catal. A 181 (1999) 71.
[8] S.M. Csisery, US Patents 3,617,488, 3,617,489, 3,617,490, 3,617,491 (1971).
[9] S. Yamanaka, G.W. Brindley, Clays Clay Miner. 27 (1979) 119.
[10] N. Lahav, U. Shani, J. Shabtai, Clays Clay Miner. 26 (1978) 107.
[11] J. Gaff, R.A. van Santen, European Patent 90,442-A2 (1983).
[12] D.E.W. Vaugan, R.J. Lussier, J.S. Magee, US Patent 4,176,090 (1979).
[13] D.E.W. Vaugan, R.J. Lussier, J.S. Magee, US Patent 4,248,739 (1981).
[14] M.L. Occelli, J.T. Hsu, L.G. Galya, J. Mol. Catal. A 33 (1985) 371.
[15] M.L. Occelli, in: S. Kaliaguine (Ed.), Selected Topics in Catalysis Research Related to Energy, Elsevier, Amsterdam, 1987.
[16] J. Shabtai, J. Fijal, US Patent 4,579,832 (1986).
[17] L. Storaro, M. Lenarda, R. Ganzerla, A. Rinaldi, Micropor. Mater. 6 (1996) 55.
[18] M.L. Occelli, R.M. Tindwa, Clays Clay Miner. 31 (1) (1983) 22.
[19] N. Maes, I. Heylen, P. Cool, E.F. Vansant, Appl. Clay Sci. 12 (1997) 43.
[20] P. Cañizares, J.L. Valverde, M.R. Sun Kou, C.B. Molina, Micropor. Mesopor. Mater. 29 (1999) 267.
[21] M.R. Sun Kou, S. Mendioroz, Thermochim. Acta 323 (1998) 145.
[22] M. Sychev, T. Shubina, M. Rozwadowski, A.P.B. Sommen, V.H.J. de Beer, R.A. van Santen, Micropor. Mesopor. Mater. 37 (2000) 187.
[23] S.M. Bradley, R.A. Kydd, J. Catal. 141 (1993) 239.
[24] N.D. Hutson, M.J. Hoekstra, R.T. Yang, Micropor. Mesopor. Mater. 28 (1999) 267.
[25] C. Flego, L. Galasso, R. Millini, I. Kirics, Appl. Catal. A 168 (1998) 323.
[26] D.E.W. Vaugan, Catal. Today 2 (1988) 187.
[27] E.P. Barret, L.G. Joyner, P.P. Halenda, J. Am. Chem. Soc. 73 (1951) 373.
[28] W.D. Harkins, G. Jura, J. Chem. Phys. 11 (1943) 431.
[29] R.A. Schoonheydt, Stud. Surf. Sci. Catal. 58 (1991) 201.
[30] K. Bukka, J. Shabtai, Clays Clay Miner. 40 (1) (1992) 92.
[31] J.D. Russell, V.C. Farmer, B. Velde, Mineralogical Mag. 37 (292) (1970) 869.
[32] V.C. Farmer, Mineralogical Soc. (1974) 331.
[33] S.J. Gregg, K.S.W. Sing, Adsorption, Surface Area and Porosity, Academic Press, New York, 1982.
[34] B.C. Lippens, J.H. de Boer, J. Catal. 4 (1965) 319.
[35] M.R. Sun Kou, S. Mendioroz, V. Muñoz, Clays Clay Miner. 48 (5) (2000) 528.
[36] S. Bodoardo, R. Chiapetta, B. Onida, F. Figueras, E. Garrone, Micropor. Mesopor. Mater. 20 (1998) 187.
[37] H. Ming Yuan, L. Zhonghui, M. Enze, Catal. Today 2 (2/3) (1988) 321.